

## One Cycle Control of Shunt Active Power Filter

**R.Nagamani**

PG Scholar,

Department of Electrical and Electronics Engineering,  
Swamy Vivekananda Engineering College,  
Kalavarai, Vizianagaram, India.

**Rajesh Satti**

Assistant Professor,

Department of Electrical and Electronics Engineering,  
Swamy Vivekananda Engineering College,  
Kalavarai, Vizianagaram, India.

### Abstract:

Non linear loads generate a harmonic and reactive current, which leads to poor power factor, low energy efficiency, and harmful disturbance to other appliances. Active Power Filters (APFs) are one of the viable solutions to eliminate the power line harmonic/reactive currents generated by nonlinear loads and improve the power factor. A shunt APF is connected in parallel with the nonlinear loads and functions as current sources to cancel the harmonic/reactive components in the line current so that the current flow into and from the grid is sinusoidal and in phase with the grid voltage. Here APF power converter is operated in dual boost converter mode with constant switching frequency by using one cycle control method with Vector operation. Here no need to calculate reference for APF inductor current so that requirement of fast acting microprocessor, complicated digital computation is eliminated. And a fuzzy logic controller is used to regulate the error signal.

### Index Terms:

Nonlinear loads, Active Power Filter (APF), Harmonic current estimation method, Dual -Boost converter, One-Cycle control, fuzzy logic controller.

### INTRODUCTION:

Nonlinear loads consist of power electronic equipment usually introduces current harmonics. These current harmonics result in problems such as Low power factor, Low efficiency Power system voltage fluctuations, Communication interference. Passive Filters consist of a bank of tuned LC filters to suppress current harmonics generated by nonlinear loads.

Passive filters easy in design, simple structure and low cost but passive filters have many disadvantages, such as Resonance, Large size, fixed compensation character, possible overload. To overcome the disadvantages due to Passive Filters, Active Power Filters (APFs) have been presented as a current-harmonic compensator.

The Active Power Filter is connected in parallel with a nonlinear load. The approach is based on the principle of injecting harmonic current into the ac system, of the same amplitude and reverse phase to that of the load current harmonics. This will thus result in sinusoidal line currents and unity power factor in the input power system. In this case, only a small portion of the energy is processed, which may result in overall higher energy efficiency and higher power processing capability.

These kinds of approaches are applicable for low-power (less than 5kVA) to high-power applications (around 100kVA). A three-phase shunt APF is typically composed of a three-phase bridge converter and control circuitry. Most of the previous control approaches need to sense the load current and calculate its harmonics and reactive components in order to generate the reference for controlling the current of a bridge converter.

Those control methods require fast and real-time calculation; therefore, a high-speed digital microprocessor and high-performance A/D converters are necessary, which yields high cost, complexity, and low stability. So here introduced a promising solution based on One-Cycle control.

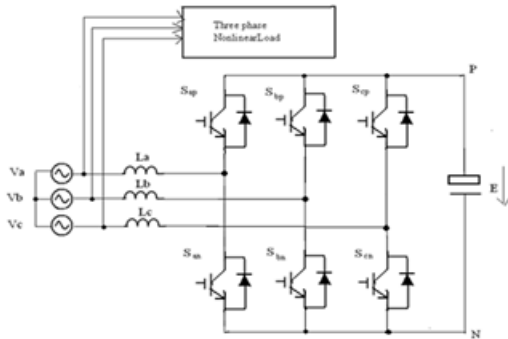


Fig.1 Power stage of the three-phase APF

The one-cycle control method eliminates the need of calculating the current reference as well as the use of multipliers in the control loop. The control circuitry is simple and reliable. In pulse width-modulation (PWM) active power filter, all switches are triggered with switching frequency; therefore, the switching losses are relatively higher than that of the vector operated active power filters. In this project, a three-phase APF with six-switch bridge voltage-source converter with vector operation is presented.

**PARALLEL CONNECTED DUAL BOOST CONVERTER:**

**Principle of operation:**

The three-phase voltage waveforms Va, Vb and Vc of the grid is shown in Fig.2. During each 60 region in Fig.2, the voltage-source converter in Fig.1 can be decoupled into a parallel-connected dual-boost converter. Here the total 360° region is divided into six regions as shown.

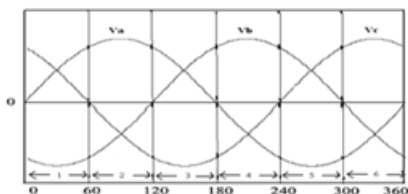


Fig.2 three-phase grid voltage waveforms

in Fig.2. In each region two voltages are either positive or negative, one voltage is either negative or positive, and depending on this condition the total 360° region is divided into six regions.

In each region the voltage-source converter is operated as a dual-boost converter as explained in the next section. In the region (0~60°), the phase voltage Vb is the lowest. In this case, switch Sbn is kept on and switch Sbp is kept off during the whole 60° region, while switches in the other two branches such as San, Sap and Scn, Scp are controlled complementally (with negligible dead time in between) at the switching frequency. For example, during each switching cycle, if switch Sap is ON, switch San will be OFF and vice versa. Here switching frequency is much higher than the line frequency. Here Switching frequency is 50 KHZ and Line frequency is 60 HZ.

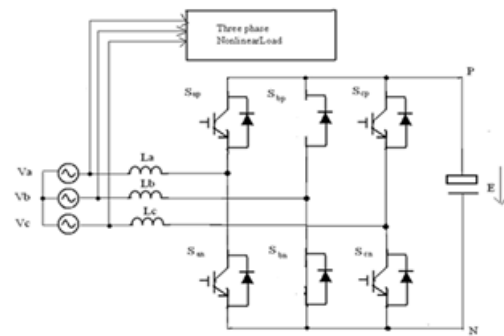


Fig.3 Power stage of the three-phase APF during 0 - 60° regions.

**Characteristics of proposed converter:**

For the dual-boost converter shown in Fig.4 or 5, four switching states are available for the two switches Tp and Tn. The four switching states and inductor voltages are shown in Table 1. Where

$$\begin{bmatrix} V_p^* \\ V_n^* \\ V_c^* \end{bmatrix} = \begin{bmatrix} \frac{2}{3} & -\frac{1}{3} \\ -\frac{1}{3} & \frac{2}{3} \\ \frac{1}{3} & \frac{1}{3} \end{bmatrix} \cdot \begin{bmatrix} V_p \\ V_n \end{bmatrix} \quad \text{-----(1)}$$

For a three-phase APF with a constant switching frequency, only two switching sequences are possible, i.e., I, II, IV (condition dp > dn, dp, dn are the duty ratios of switches,

State	T <sub>p</sub>	T <sub>n</sub>	T <sub>p</sub>	T <sub>n</sub>	V <sub>Lp</sub>	V <sub>Ln</sub>	V <sub>Lt</sub>
I	ON	ON	OFF	OFF	V <sub>p</sub> <sup>*</sup>	V <sub>n</sub> <sup>*</sup>	V <sub>t</sub> <sup>*</sup>
II	ON	OFF	OFF	ON	V <sub>p</sub> <sup>*</sup> + 1/3 E	V <sub>n</sub> <sup>*</sup> - 2/3 E	V <sub>t</sub> <sup>*</sup> - 1/3 E
III	OFF	ON	ON	OFF	V <sub>p</sub> <sup>*</sup> - 2/3 E	V <sub>n</sub> <sup>*</sup> + 1/3 E	V <sub>t</sub> <sup>*</sup> - 1/3 E
IV	OFF	OFF	ON	ON	V <sub>p</sub> <sup>*</sup> - 1/3 E	V <sub>n</sub> <sup>*</sup> - 1/3 E	V <sub>t</sub> <sup>*</sup> - 2/3 E

T<sub>p</sub>, T<sub>n</sub> respectively) or I, III, IV (condition d<sub>p</sub> < d<sub>n</sub>) during each switching cycle, if trailing-edge modulation is performed. The voltage waveforms across inductors L<sub>p</sub>, L<sub>n</sub>, L<sub>t</sub> are shown in Fig.6 for the first switching sequence (d<sub>p</sub> > d<sub>n</sub>). Based on the assumption that switching frequency is much higher than the line frequency, the inductor voltage-second balance is approximately valid, that is

$$\left. \begin{aligned} V_p^* d_p + (V_p^* + \frac{1}{3}E)(\phi_p - d_n) + (V_p^* - \frac{1}{3}E)(1 - \phi_p) &= 0 \\ V_n^* d_n + (V_n^* - \frac{2}{3}E)(\phi_p - d_n) + (V_n^* + \frac{1}{3}E)(1 - \phi_p) &= 0 \\ V_t^* d_n + (V_t^* - \frac{1}{3}E)(\phi_p - d_n) + (V_t^* - \frac{2}{3}E)(1 - \phi_p) &= 0 \end{aligned} \right\} \text{---(2)}$$

The following equation is true for a symmetrical three-phase system:

$$V_p^* + V_n^* - V_t^* = 0 \text{ ---(3)}$$

From (2) and (3) with further simplification we will get

$$\begin{bmatrix} (1 - \phi_p) \\ (1 - \phi_n) \end{bmatrix} = \begin{bmatrix} 2 & 1 \\ 1 & 2 \end{bmatrix} \cdot \begin{bmatrix} \frac{V_p^*}{E} \\ \frac{V_n^*}{E} \end{bmatrix} \text{---(4)}$$

It has been verified that this equation is valid for the other switching sequence I, III, and IV (d<sub>p</sub> < d<sub>n</sub>) as well. Equation (4) gives an inherent relationship between the duty cycle and the input, output voltage for the parallel-connected dual-boost converter.

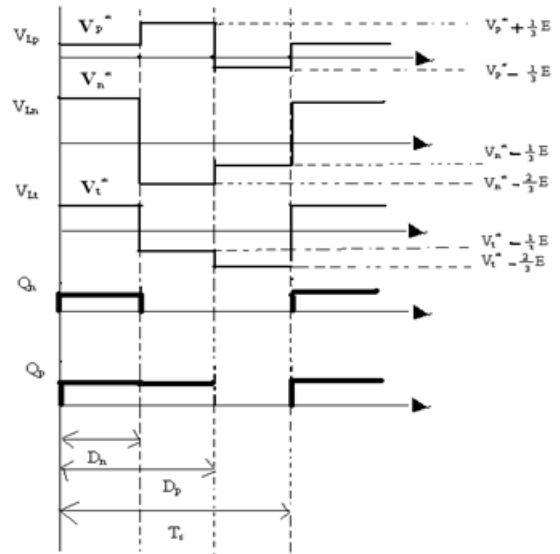


**Fig.4 Inductor voltage waveforms for the converter under the condition d<sub>p</sub> > d<sub>n</sub>**

In Fig.6 V<sub>Lp</sub>, V<sub>Ln</sub>, and V<sub>Lt</sub> represents the voltage across inductors V<sub>p</sub>, V<sub>n</sub>, and V<sub>t</sub>, respectively. Q<sub>p</sub> and Q<sub>n</sub> are driving signals for switches T<sub>p</sub> and T<sub>n</sub> respectively.

**PROPOSED ONE-CYCLE CONTROLLER FOR THREE-PHASE APF**

For the unity-power-factor three-phase APF, the control goal is to force the grid line current in each phase to follow the correspondent sinusoidal phase voltage, i.e.,

$$\left. \begin{aligned} V_a &= Re \cdot i_a \\ V_b &= Re \cdot i_b \\ V_c &= Re \cdot i_c \end{aligned} \right\} \text{---(5)}$$

where Re is the emulated resistance that reflects the real power of the load. This control goal can be realized by controlling the equivalent currents i<sub>p</sub> and i<sub>n</sub> to follow the voltages V<sub>p</sub><sup>\*</sup> and V<sub>n</sub><sup>\*</sup>. The control goal of three-phase APF can be rewritten as

$$\left. \begin{aligned} V_p^* &= Re \cdot i_p \\ V_n^* &= Re \cdot i_n \end{aligned} \right\} \text{---(6)}$$

Substituting (6) into (4) and considering the switch is ON for the entire 60 region, it is obtained that

$$\begin{bmatrix} (1-d_p) \\ (1-d_n) \end{bmatrix} = \frac{R_e}{E R_s} \cdot R_s \cdot \begin{bmatrix} 2 & 1 \\ 1 & 2 \end{bmatrix} \cdot \begin{bmatrix} i_p \\ i_n \end{bmatrix} \quad d_n=1 \quad (7)$$

Define

$$V_m = \frac{E R_s}{R_e} \quad (8)$$

where the signal  $V_m$  can be generated from the output voltage feedback compensator, which is used to regulate the output capacitor voltage  $E$  of the voltage source converter according to the load level;  $R_s$  is equivalent current sensing resistance and it is fixed constant. Combining of the two equations 7,8 and the control key equation is derived as

$$V_m \cdot \begin{bmatrix} (1-d_p) \\ (1-d_n) \end{bmatrix} = R_s \cdot \begin{bmatrix} 2 & 1 \\ 1 & 2 \end{bmatrix} \cdot \begin{bmatrix} i_p \\ i_n \end{bmatrix} \quad d_n=1 \quad (9)$$

The above equation indicates that three-phase power factor can be achieved by controlling the duty ratios of switches so that first-order polynomial equation (9) is satisfied. This can be realized by the one-cycle control core as shown in Fig.7. The operation waveforms are shown in Fig.8.

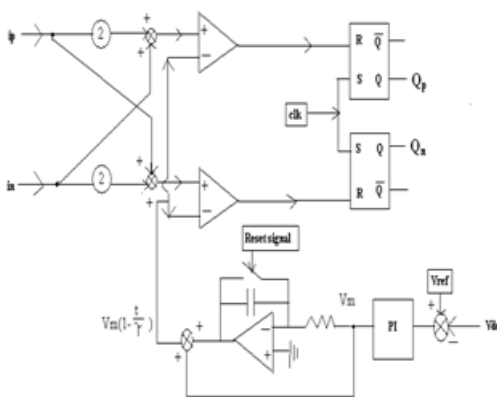


Fig.5 One-cycle control logic

In the beginning of each switching cycle, the clock pulse sets the two flip-flops. The currents  $i_p$  and  $i_n$  from the current selection logic is linearly combined to form an input to each of the two comparators.

At other input of the two comparators is the value of  $V_m$  minus the integrated value of  $V_m$ . Signal  $V_m(1-t/T_s)$  is compared with  $R_s(2 i_p + i_n)$  in the upper comparator and is compared with  $R_s(i_p + 2 i_n)$  in the lower comparator as shown in Fig.7. When the two inputs of a comparator meet as shown in Fig.8, the comparator changes its state, which resets the correspondent flip-flop. As a result, the correspondent switch is turned off. Therefore, the duty ratios  $d_p$  and  $d_n$  are determined for the correspondent switch in each switching cycle.

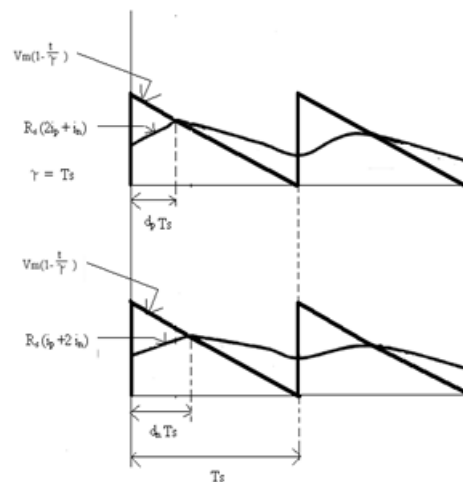


Fig.6 Operation waveforms of One-cycle controlled APF controller

**The Presented One-Cycle Control Approach has the Following Features**

- Three-phase unity-power-factor and low total harmonic distortion (THD) are achieved by one integrator with reset as well as several logic and linear components. It is simple and reliable.
- Only ac mains current and voltage zero-crossing points are sensed. No sensors for the load current and the APF inductor current are required.
- There is no need to calculate the reference for APF inductor current so that complicated digital computation is eliminated.
- No multipliers are required.
- Constant switching frequency, which is desirable for industrial applications, is achieved.
- For the three-phase bridge converter, only two switches are operated in high frequency, and

switching losses are reduced compared to PWM-operated ones.

**DESIGN CONSIDERATION**

**Dc-Link Capacitor Design**

The output dc-link capacitor of voltage source converter is determined by the output voltage ripple. The equation is given by

$$C \geq \frac{P_o}{2 * f_{line} * (V_{omax}^2 - V_{omin}^2)} \text{ ----- (10)}$$

For example, suppose the power is 7000 W; APF and output voltage is 400 V with 2% ripple. The line frequency is 60 Hz. The capacitance is calculated as 4800µF.

**Selection of APF Inductance**

The concept of the proposed control is using one-cycle control to implement the control key equation as follows:

$$R_s \cdot i_{eq} = V_m \cdot (1-d) \text{ -----(11)}$$

Where

$$i_{eq} = (2i_p + i_n) \text{ (OR)} \quad (i_p + 2 i_n)$$

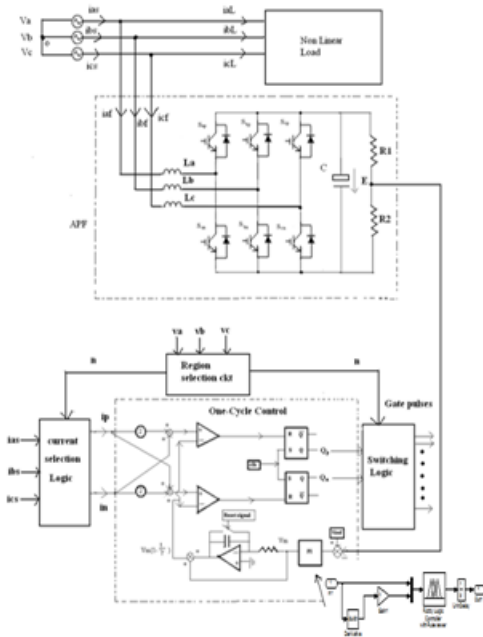


**Fig.7 Block diagram of One-Cycle controlled APF with PI and Fuzzy controllers**

The operation waveforms are shown in Fig.9. Similar to the peak current model control, there is the convergence condition. The stability condition is given by

$$m_c \geq \frac{(m_2 - m_1)}{2} \text{ ----- (12)}$$

where  $m_1$  is the ON slope of the input current and  $m_2$  is the OFF slope of the input current;  $m_c$  is the equivalent slope of the carrier signal, which is implemented by integrator with reset. Considering that the load current is low frequency and the influence of load current can be neglected, we only concern the inductor current in the stability analysis, we have

$$\begin{aligned} m_1 &= R_s \cdot \frac{V_g}{L} \\ m_2 &= R_s \cdot \frac{V_o - V_g}{L} \text{ ----- (13)} \\ m_c &= \frac{V_m}{\gamma} = \frac{V_m}{T_s} \end{aligned}$$

Where

$$\gamma = T_s$$

Substitution of (13) into (12) yields the convergence condition

$$\begin{aligned} V_m &\geq \frac{R_s \cdot T_s}{2L} \cdot (V_o - 2|V_g|) \text{ ----- (14)} \\ &\geq \frac{R_s \cdot T_s}{2L} \cdot (V_o - 2 \cdot V_{gms} |\sin(\omega t)|) \end{aligned}$$

He convergence condition is dependent on the angular angle of “ input voltage  $\omega t$  and the  $V_m$ , which is related to the output power and input voltage. When the convergency condition is satisfied partially, the system will still be stable. According to (14), convergence condition for region  $0^\circ \sim 360^\circ$  is given by

$$V_m \geq \frac{R_s \cdot T_s}{2L} \cdot V_o \text{ ----- (15)}$$

But

$$V_m = \frac{V_o R_s}{R_e} \text{ -----(16)}$$



$V_m$  is related to input voltage and output power through (16) . It can be rewritten as

$$V_m = \frac{P_o \cdot R_s \cdot V_o}{\eta \cdot V_{grms}^2} \text{ -----(17)}$$

where  $\eta$  is the estimated efficiency.

Combination of the above equations yields

$$L \geq \frac{1}{2} \cdot \eta \cdot T_s \cdot \frac{V_{grms}^2}{P_o} \text{ -----(18)}$$

The above equation was used to determine the size of inductor. At full load and maximum input voltage condition, the system should be fully stable, then the inductor can be selected by

$$L \geq \frac{1}{2} \cdot \eta \cdot T_s \cdot \frac{\max(V_{grms}^2)}{\max(P_o)} \text{ -----(19)}$$

For  $\eta=90\%$  ,  $T_s=20\mu s$ ,  $\max(V_{grms})=170$  v,  $\max(P_o)=7000W$  then the minimum inductance is calculated as  $L = 250\mu H$ .

## V FUZZY LOGIC CONTROLLERS

### Introduction To Fuzzy Logic:

The logic of an approximate reasoning continues to grow in importance, as it provides an inexpensive solution for controlling known complex systems. Fuzzy logic controllers are already used in appliances washing machine, refrigerator, vacuum cleaner etc. Computer subsystems (disk drive controller, power management) consumer electronics (video, camera, battery charger) C.D. Player etc. and so on in last decade, fuzzy controllers have converted adequate attention in motion control systems. As they later possess non-linear characteristics and a precise model is most often unknown. Remote controllers are increasingly being used to control a system from a distant place due to inaccessibility of the system or for comfort reasons. In this work a fuzzy remote controller is developed for speed control of a converter fed dc motor. The performance of the fuzzy controller is compared with conventional P-I controller.

## VI SIMULATION RESULTS:

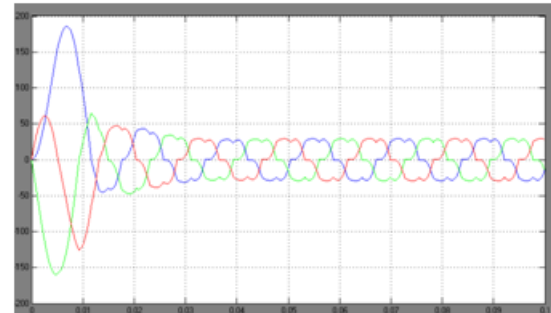


**Fig.8 Source current without APF**

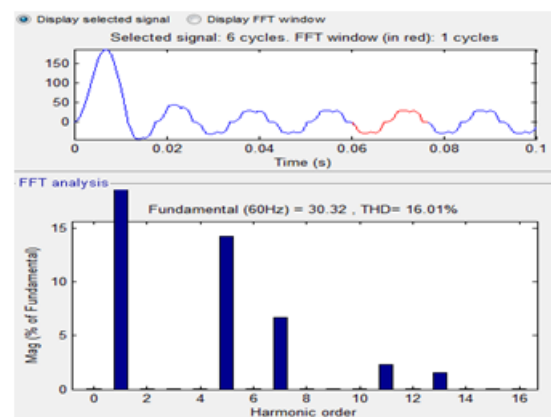


**Fig.9 THD without APF**

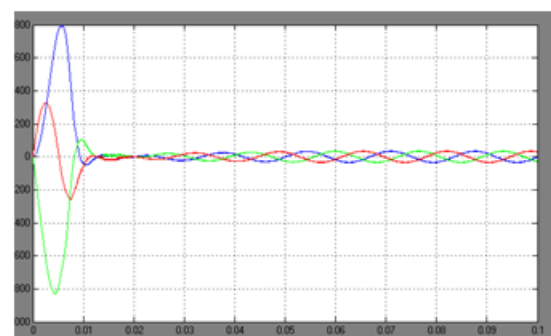


**Fig.10 Source current with fuzzy one cycle control**

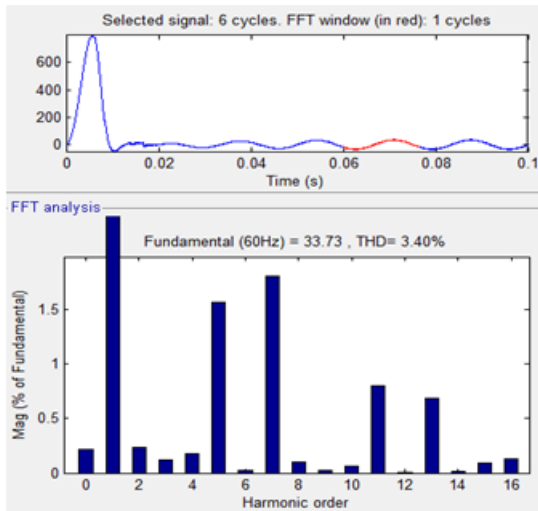


Fig.11 THD with pi one cycle controller

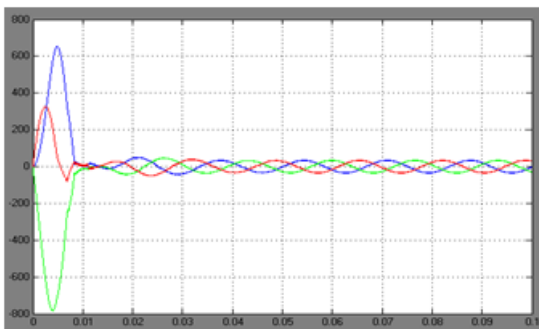


Fig.12 Source current with fuzzy one cycle control

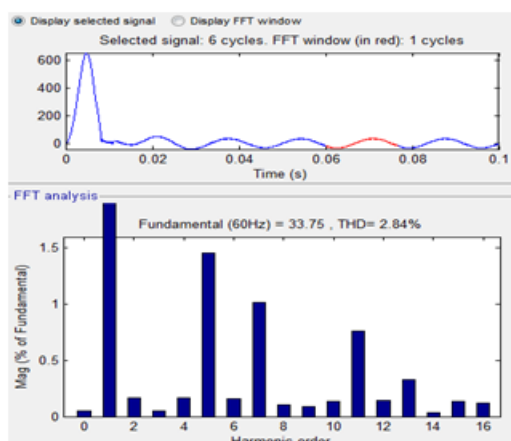


Fig.13 THD with fuzzy one cycle controller

## VII CONCLUSION:

In this paper, a three-phase APF with fuzzy one-cycle control has been proposed. The proposed control approach senses only the mains current and the zero

crossing of grid voltage. Furthermore, there is no need to calculate the reference for APF inductor current so that the intensive digital computation is eliminated. A non linear load is connected to a distribution system which produces harmonics in the source. In order to reduce the harmonics a fuzzy logic one cycle control APF is connected in parallel to the system. The total harmonic reduction without APF - 16.1% and with PI - 3.40% and with Fuzzy - 2.84%. hence the harmonics are reduced using fuzzy logic controller APF.

## VIII REFERENCES:

- [1] G. O. Young, "Synthetic structure of industrial plastics (Book style with paper title and editor)," in *Plastics*, 2nd ed. vol. 3, J. Peters, Ed. New York: McGraw-Hill, 1964, pp. 15–64.
- [2] W.-K. Chen, *Linear Networks and Systems* (Book style). Belmont, CA: Wadsworth, 1993, pp. 123–135.
- [3] H. Poor, *An Introduction to Signal Detection and Estimation*. New York: Springer-Verlag, 1985, ch. 4.
- [4] B. Smith, "An approach to graphs of linear forms (Unpublished work style)," unpublished.
- [5] E. H. Miller, "A note on reflector arrays (Periodical style—Accepted for publication)," *IEEE Trans. Antennas Propagat.*, to be published.
- [6] J. Wang, "Fundamentals of erbium-doped fiber amplifiers arrays (Periodical style—Submitted for publication)," *IEEE J. Quantum Electron.*, submitted for publication.
- [7] C. J. Kaufman, Rocky Mountain Research Lab., Boulder, CO, private communication, May 1995.
- [8] Y. Yorozu, M. Hirano, K. Oka, and Y. Tagawa, "Electron spectroscopy studies on magneto-optical media and plastic substrate interfaces(Translation Journals style)," *IEEE Transl. J. Magn.Jpn.*, vol. 2,



Aug. 1987, pp. 740–741 [Dig. 9th Annu. Conf. Magnetism Japan, 1982, p. 301].

[9] M. Young, *The Technical Writers Handbook*. Mill Valley, CA: University Science, 1989.

[10] J. U. Duncombe, “Infrared navigation—Part I: An assessment of feasibility (Periodical style),” *IEEE Trans. Electron Devices*, vol. ED-11, pp. 34–39, Jan. 1959.

[11] S. Chen, B. Mulgrew, and P. M. Grant, “A clustering technique for digital communications channel equalization using radial basis function networks,” *IEEE Trans. Neural Networks*, vol. 4, pp. 570–578, July 1993.

[12] R. W. Lucky, “Automatic equalization for digital communication,” *Bell Syst. Tech. J.*, vol. 44, no. 4, pp. 547–588, Apr. 1965.

[13] S. P. Bingulac, “On the compatibility of adaptive controllers (Published Conference Proceedings style),” in *Proc. 4th Annu. Allerton Conf. Circuits and Systems Theory*, New York, 1994, pp. 8–16.

[14] G. R. Faulhaber, “Design of service systems with priority reservation,” in *Conf. Rec. 1995 IEEE Int. Conf. Communications*, pp. 3–8.

[15] W. D. Doyle, “Magnetization reversal in films with biaxial anisotropy,” in *1987 Proc. INTERMAG Conf.*, pp. 2.2-1–2.2-6.